High Energy Processes in Accreting Black Holes
ASP Conference Series, Vol. 161, 1999
Juri Poutanen and Roland Svensson, eds.

X-rays and Soft Gamma-rays from Seyferts, Radio Galaxies, and Black-Hole Binaries

Andrzej A. Zdziarski

N. Copernicus Astronomical Center, Bartycka 18, 00-716 Warsaw, Poland

Abstract. Selected topics dealing with X-ray/soft γ-ray emission from accreting black-hole sources are reviewed. The shape of soft γ-ray spectra of Seyferts observed by OSSE can be well modeled by thermal Comptonization. A very strong correlation between the X-ray slope and the strength of Compton reflection in these sources can then be explained by thermal Comptonization in vicinity of the reflecting cold media. Similar correlation is seen for the hard state of black-hole binaries, but the strength of Compton reflection at a given X-ray slope is larger than in Seyferts. This appears to be due to seed photons (for Comptonization) emitted by the cold media having larger energies in stellar-mass systems than in Seyferts. Broad-line radio galaxies have hard X-ray spectra with weak reflection, which reflection is similar to that in Seyferts with hard X-ray spectra. Two main models for the source geometry, a hot inner disk surrounded by a cold outer disk, and a dynamic corona above a cold disk, appear about equally viable based on the presently available data.

1. Introduction

The origin of X-rays and soft γ-rays (hereafter Xγ) from accreting black-hole sources has been a major problem of high-energy astrophysics for many years. Currently, we can probably identify main radiative processes taking place in those sources, but their geometry and dynamics remain still unknown.

In this paper, I first present a short general discussion of various classes of Xγ sources around accreting black holes. This is followed by discussion in more detail of selected specific topics: soft γ-ray spectra of Seyferts, Compton reflection, and Xγ emission from broad-line radio galaxies (hereafter BLRGs), with emphasis on radiative processes giving rise to observed spectra. Finally, I discuss some constraints on geometry of the sources. Recent related reviews include Poutanen (1998) and Zdziarski et al. (1997, hereafter Z97).

2. Overview

We can distinguish the following classes of X-ray sources powered by accretion onto a black hole. First, there are black-hole binaries, which have either persistent or transient X-ray sources. These sources are in one of two main spectral states: a soft (also called high) one or a hard (also called low) one, and they

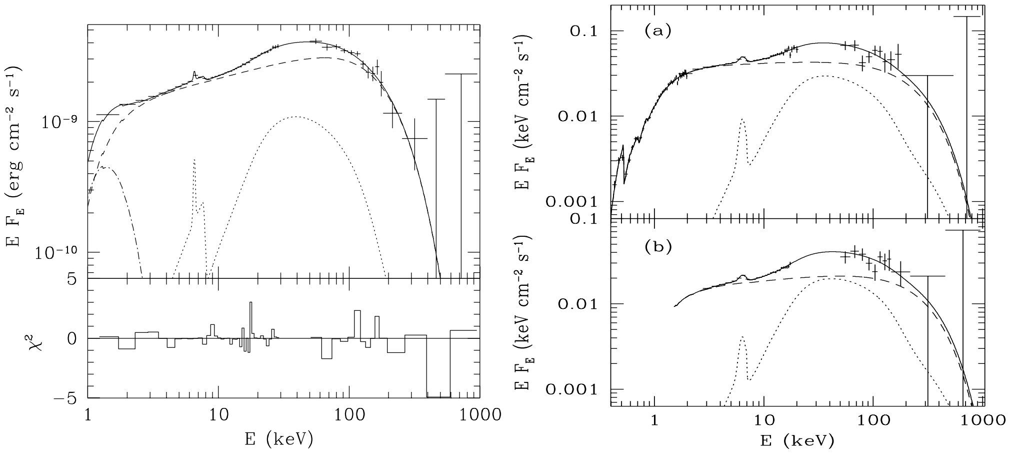

Figure 1. The Xγ spectra of GX 339–4 (a black-hole binary) in the hard state (left panel), of IC 4329A, a Seyfert 1 (right upper panel), and of the average of 5 Seyfert 1s detected by both *Ginga* and OSSE (right lower panel). The solid curves correspond to models consisting of thermal Comptonization in a plasma with $kT \sim 10^2$ keV and $\tau \sim 1$ (dashes), a reprocessed component with a Compton-reflection continuum and a fluorescent Fe Kα line (dots), and, in the case of GX 339–4, a soft blackbody emission (a dot-dashed curve).

often switch between the states. Then radio-quiet (hereafter RQ) Seyfert 1s are nearby AGNs without strong jets and observed without strong obscuration. Xγ spectra of Seyfert 1s are remarkably similar to Xγ spectra of black-hole binaries in the hard state. Seyfert 2s, most likely, belong to the same intrinsic class as Seyfert 1s, but are oriented close to edge-on, which results in strong obscuration both in the optical/UV and X-ray ranges. Finally, radio galaxies form a rather enigmatic X-ray class, with their X-ray properties somewhat similar to those of Seyferts.

A distinct class appears to be formed by Narrow-Line Seyfert 1s, whose X-ray spectra are very soft, and within observational uncertainties, similar to those of black-hole binaries in the soft state (Pounds, Done & Osborne 1995). However, very little is known about their hard X-ray and soft γ-ray properties.

Hard X-ray spectra of basically all the considered classes of sources consist of (intrinsic) power laws (with the photon number flux $\propto E^{-\Gamma}$ and typical spectral indices of $\Gamma \sim 1.5$–3) accompanied, in most cases, by signatures of reprocessing by cold media: Fe Kα lines (e.g. George & Fabian 1991) and Compton reflection (Lightman & White 1988; Magdziarz & Zdziarski 1995).

The intrinsic hard X-ray power laws often break at ~ 100 keV. The form of the spectra in that range is known most accurately for black-hole binaries. Their spectra in the hard state show high-energy breaks with a characteristic curvature (Grove et al. 1998), which is well modeled by thermal Comptonization in a plasma with a temperature, $kT \sim 100$ keV, and a Thomson optical depth, $\tau \sim 1$ (Gierliński et al. 1997; Zdziarski et al. 1998, hereafter Z98). A typical example of such a spectrum is that of of the hard state of GX 339–4, a black hole candidate, shown in the left panel of Fig. 1 (Z98).

On the other hand, no distinct high-energy cutoffs are seen in the soft state of black-hole binaries up to ~ 1 MeV (Grove et al. 1998; Phlips et al. 1996; Tomsick et al. 1999). This lack of cutoffs in soft γ-rays is likely a signature of Compton scattering by non-thermal, relativistic, electrons with a distribution close to a power law (Poutanen & Coppi 1998; Gierliński et al. 1999).

Due to the relative weakness of their observed soft γ-ray fluxes, the shape of high-energy cutoffs of AGNs is known much less accurately. Still, NGC 4151, the RQ Seyfert brightest in soft γ-rays, has intrinsic Xγ spectra well modeled by thermal Comptonization in a plasma with kT and τ very similar to those of black-hole binaries (Zdziarski, Johnson & Magdziarz 1996; Johnson et al. 1997a). Two examples of broad-band Xγ spectra of Seyfert 1s are shown in Fig. 1 (Z97). The right top panel shows a spectrum of the Seyfert 1 IC 4329A, and the right bottom panel shows the average spectrum of 5 Seyfert 1s detected by both *Ginga* and *CGRO*/OSSE (Gondek et al. 1996), both fitted with a model consisting of thermal Comptonization and Compton reflection. Also, the average spectra of all RQ Seyfert 1s and 2s detected by OSSE show a similarly curved shape as the spectrum of NGC 4151 (Z97; §3 below).

The shape of soft γ-ray spectra of radio galaxies is known even less accurately. On one hand, their Xγ spectra do show breaks at ~ 100 keV (Woźniak et al. 1998, hereafter W98), but, on the other hand, the soft γ-ray spectra above the break are compatible with a power-law form, without evidence for further curvature. The Xγ spectrum of the brightest radio galaxy, Cen A, shows a similar break at ~ 100 keV with a power law above this break continuing up to > 10 MeV, and with some flux detected even at $\gtrsim 100$ MeV (Steinle et al. 1998). Such spectrum is incompatible with thermal Comptonization, and its modeling seems to require non-thermal processes similar to those operating in blazars.

In soft X-rays, all these classes of sources show additional components above extrapolation of the hard X-ray power laws to lower energies. In Seyferts and radio galaxies, such soft X-ray excesses are common below ~ 1 keV. Typically, the intrinsic soft X-ray spectra are power-law like and, when extrapolated to the UV range, join onto the observed UV spectra, see, e.g. Magdziarz et al. (1998).

Black-hole binaries show additional soft X-ray components as well. For example, Cyg X-1 in the hard state shows a blackbody component with a temperature of ~ 0.15 keV together with a soft power-law component intersecting the hard X-ray power law at ~ 3 keV (Ebisawa et al. 1996). In the soft state, the blackbody temperature is higher, e.g. ~ 0.4 keV in the case of Cyg X-1, but an additional soft-excess component in addition to both the blackbody and the hard X-ray power law is still present (Gierliński et al. 1999).

The interpretation of the soft power-law excesses present in both Seyferts and both spectral states of black-hole binaries remains relatively unclear. Plausibly, they are due to Comptonization by a thermal plasma with a small Compton parameter $[y \equiv 4(kT/m_{\rm e}c^2)\max(\tau,\tau^2) \ll 1]$ in addition to Comptonization by another plasma forming the hard X-ray power law (e.g. Magdziarz et al. 1998; Gierliński et al. 1999). On the other hand, the blackbody component in black-hole binaries and the blue-bump UV component in Seyferts originate likely in an optically-thick accretion disk.

Finally, the observed spectra are attenuated by bound-free absorption due to the Galactic column density towards the source. Also, intrinsic absorption by

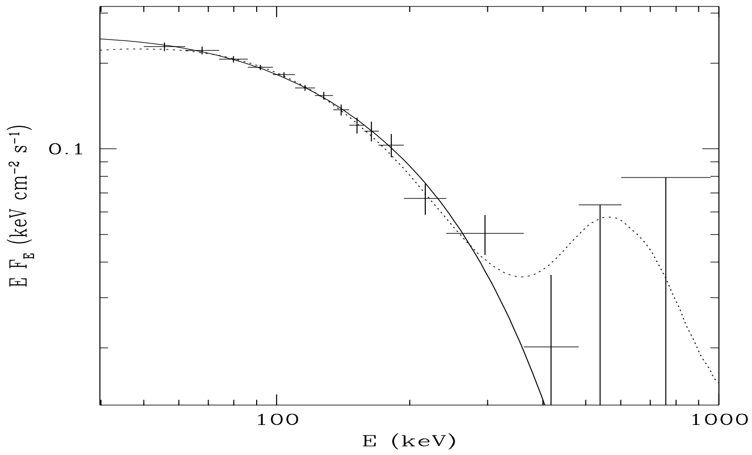

Figure 2. The average OSSE spectrum of NGC 4151. The solid curve represents the best-fit thermal-Comptonization model. The dotted curve corresponds to a hybrid thermal/non-thermal model with the maximum allowed fraction ($\approx 15\%$) of the total power going into electron acceleration (with the remainder used for electron heating).

both neutral and ionized matter is commonly seen in AGNs. On the other hand, intrinsic absorption in black-hole binaries is typically transient (e.g. in Cyg X-1, Ebisawa et al. 1996).

3. Soft Gamma-ray Spectra of Seyferts

As stated in §2, intrinsic broad-band Xγ spectra of Seyferts are well modeled by thermal Comptonization with $kT \sim 10^2$ keV and $\tau \sim 1$. These parameters are implied by the shape of high-energy cutoffs observed in soft γ-rays by OSSE when combined with the spectra observed in X-rays. Soft γ-ray spectra of Seyferts from OSSE are reviewed by Johnson et al. (1997b). The OSSE spectra are limited in photon statistics, and significant constraints can thus be obtained for brightest objects and average spectra only.

The RQ Seyfert brightest in soft γ-rays, NGC 4151, was studied by Zdziarski et al. (1996) and Johnson et al. (1997a). They found that its Xγ spectra are well modeled by thermal Comptonization in a plasma with $kT \sim 60$ keV and $\tau \sim 1$. These data can also be used to constrain a possible presence of non-thermal electrons in the source. A fraction of the total power in the source going to acceleration of electrons to suprathermal energies is $\lesssim 15\%$ (and consistent with null), as illustrated in Fig. 2. Interestingly, the average OSSE spectrum of NGC 4151 is virtually identical in shape to the 1991 September OSSE spectrum of GX 339–4, a black-hole candidate (Z98; see Fig. 1 above).

We then consider co-added spectra of all RQ Seyfert 1s and of all Seyfert 2s detected by OSSE through 1998 January (Zdziarski, Poutanen & Johnson, in preparation). This represents a significant update of the average OSSE spectra detected through 1995, which were presented in Z97. The Seyfert-1 average spectrum has been obtained by combining 1.4×10^7 seconds of OSSE exposure

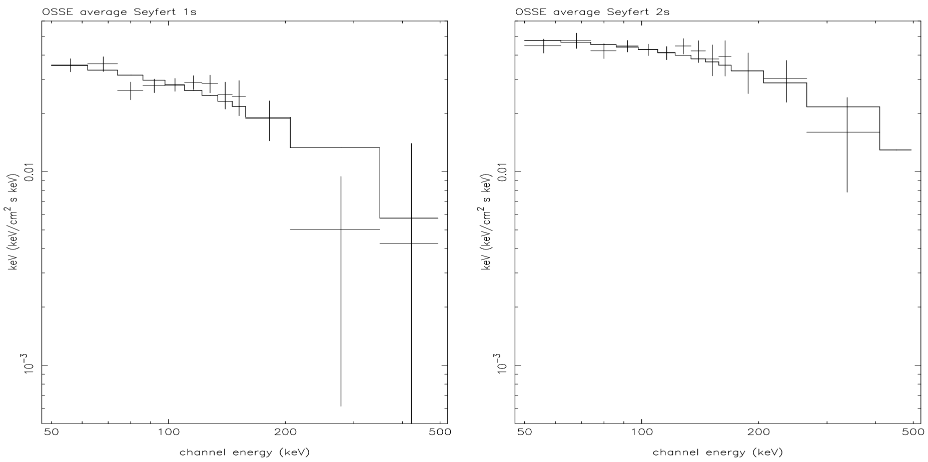

Figure 3. The average OSSE spectra of Seyfert 1s and 2s, fitted by thermal Comptonization and Compton reflection.

(scaled to a single OSSE detector) of 17 AGNs: ESO 141–55, IC 4329A, III Zw 2, MCG +8-11-11, MCG –2-58-22, MCG –6-30-15, Mkn 279, Mkn 509, Mkn 841, NGC 3227, NGC 3516, NGC 3783, NGC 526 A, NGC 5548, NGC 6814, NGC 7213, NGC 7469. The Seyfert-2 average spectrum has been obtained by combining 8.2×10^6 seconds of exposure of 10 AGNs: MCG –5-23-16, Mkn 3, NGC 1275, NGC 2110, NGC 4388, NGC 4507, NGC 4945, NGC 5506, NGC 7172, NGC 7582.

We fit the spectra, shown in Fig. 3, in the 50–500 keV range. First, we find a significant presence of high-energy cutoffs in the average spectra. Namely, the χ^2_ν improves from 33/35 and 48/35 for power-law fits to 25/34 and 34/34 for fits with an e-folded power law in the case of the Seyfert-1 and Seyfert-2 average spectrum, respectively. The statistical significance of the presence of spectral curvature corresponds then to the probability that the fit improvement were by chance of 0.002 and 0.0007 for Seyfert 1s and 2s, respectively. This result argues strongly that the spectra of individual Seyferts are strongly cut off as well. If, instead, their spectra were simple power laws with a range of spectral indices, the sum spectrum would have a concave shape rather than the observed convex one.

We then consider models with thermal Comptonization and Compton reflection. We find that the OSSE data alone cannot constrain the spectral index in the X-ray range as well as the strength of reflection. Therefore, we first use the average Xγ spectrum of Seyfert 1s observed by both *Ginga* and OSSE of Gondek et al. (1996) (shown on the lower right panel of Fig. 1). We fit that spectrum with a model of thermal Comptonization in a hot plasma slab with sources of seed photons located in the midplane (Z98). We assume the inclination of a surrounding (reflecting) cold disk of $i = 30^\circ$, as expected for Seyfert 1s (e.g. Nandra et al. 1997). We then use the Compton y parameter, $y = 0.25$ [$y \equiv 4(kT/m_{\rm e}c^2)\tau$, which corresponds to $\Gamma \approx 1.9$] and the relative reflection strength obtained from that fit in fitting our average spectrum of all Seyfert 1s detected by OSSE. (Although the OSSE data alone only weakly constrain y,

$y = 0.25$ is within 1σ of the best fit.) This gives the optical depth corresponding to the half-thickness of the slab of $\tau = 0.33^{+0.07}_{-0.08}$, which implies $kT = 100^{+30}_{-20}$ keV (at $y = 0.25$). This spectrum is shown in the left panel of Fig. 3. We also consider another geometry, of central hot sphere surrounded by a cold disk partly embedded in the sphere (Poutanen, Krolik & Ryde 1997). For this geometry, the best-fit radial optical depth of the central sphere is $\tau = 1.3$.

Similar results are obtained for the average spectrum of Seyfert 2s (see the right panel of Fig. 3), for which we also assume $y = 0.25$ and the relative strength of Compton reflection as for Seyfert 1s except that now $i = 60°$. Then the optical depth of the half-thickness of the slab is $\tau = 0.25^{+0.07}_{-0.06}$, corresponding to $kT = 130^{+30}_{-30}$ keV and to the radial optical depth of the central sphere of $\tau = 1.1$. We see that the average plasma parameters of Seyfert 1s and 2s overlap within 90% confidence, consistent with the unified AGN model.

4. Hard X-ray Power Laws and Compton Reflection

Compton reflection (Lightman & White 1988) is a process of backscattering of Xγ radiation from a cold medium subtending some solid angle when viewed from the primary source. Compton reflection of a power-law spectrum produces a characteristic spectral hump peaking at a few tens of keV, which is due to bound-free absorption of the incident radiation below ~ 10 keV and the inelasticity of Compton scattering above ~ 100 keV. Compton reflection can be measured by a relative normalization, R, of the *observed* reflected component with respect to the primary one, where $R = 1$ corresponds to reflection of an isotropic source from an infinite slab. If the primary source is isotropic and neither the source nor the reflector are obscured, $R = \Omega/2\pi$, where Ω is the solid angle subtended by the reflector as viewed from the primary source.

Note that in many situations $R \neq \Omega/2\pi$. First, the primary source may be strongly obscured but a part of the reflector is directly visible, e.g., in Seyfert 2s, in which case we may have a reflection-dominated spectrum with $R \gg 1$ (e.g. Reynolds et al. 1994). Also, the primary source may be not isotropic in the reflector frame (Ghisellini et al. 1990; Beloborodov 1999a, hereafter B99a), which may either increase or decrease R with respect to the isotropic case. Furthermore, the reflected component may be Compton-scattered in the primary source (Poutanen & Svensson 1996; Z98), which reduces the observed R. These distinctions should be kept in mind when comparing an observed strength of reflection, R, to a solid angle, Ω, inferred in a model.

Thus, R is a quantity much more model-independent than Ω. A remaining uncertainty in fitted values of R is due to its dependence on the viewing angle, i, of the reflecting plane, which is not known accurately for most Xγ sources. In general, the intensity of the reflected radiation decreases with increasing i. Furthermore, there is some dependence of reflected spectra on geometry. Below, we assume reflection as for an isotropic irradiation of a slab (but with R as a free parameter), for which case viewing-angle dependent Green's functions are given by Magdziarz & Zdziarski (1995).

Continuum signatures of Compton reflection have been discovered in all of the classes of sources considered here (Pounds et al. 1990; Nandra & Pounds 1994; Done et al. 1992; Ueda et al. 1994; Ebisawa et al. 1996; Gierliński et al.

1999; Tomsick et al. 1999). Also Compton reflection has been found in spectra of some weakly-magnetized neutron-star binaries (Yoshida et al. 1993; Strickman et al. 1996) and white-dwarf binaries (e.g. Done, Osborne & Beardmore 1995; Done & Osborne 1997; Done & Magdziarz 1998; Cropper, Ramsey & Wu 1998).

A very strong correlation of the strength of Compton reflection with the spectral index of the intrinsic spectrum, Γ, in both Seyferts and X-ray binaries in the hard state has been found by Zdziarski, Lubiński & Smith (1999, hereafter ZLS99). Fig. 4 shows their results (with addition of data for Nova Muscae 1991) for RQ Seyferts and X-ray binaries in the hard state. The observations used are by *Ginga*. We see that all the contours occupy a well-defined strip in the (Γ, R) parameter space, with the hardest spectra having almost no reflection and then with R increasing with Γ. The softest Seyfert in the sample, MCG –6-30-15 (with $\Gamma \sim 2.5$) has somewhat less reflection that would be expected from extrapolation from harder spectra. Possibly, the reflection strength in Seyfert 1s saturates at $R \sim 2$.

From Fig. 4, we see that the error contours for individual spectra typically span a much shorter range in the (Γ, R) space than the extent of the correlation itself. Thus, the correlation cannot be an artifact of the fitting method. This is confirmed by a detailed statistical analysis performed in ZLS99 using a method of Brandt (1997), which yields the significance of the physical correlation alone (i.e., after removing the effect of the measurement-related individual correlations) for the subsample of RQ Seyferts of $> (1 - 2 \times 10^{-10})$. We note that spectra of Seyferts from *RXTE* published so far (MCG –5-23-16, Weaver, Krolik & Pier 1998; MCG –6-30-15, Lee et al. 1998) show values of (Γ, R) within the area outlined by the Seyfert confidence contours in Fig. 4a, i.e., consistent with the results of ZLS99.

As shown in ZLS99, correlations very similar to the global one are seen in multiple observations of some individual objects. Fig. 4b shows the correlation for NGC 5548, which was earlier found by Magdziarz et al. (1998). The presence of this correlation represents a strong argument against the global correlation being an orientation effect, as a change of the orientation of an AGN on a short time scale (days in the case of NGC 5548) is highly unlikely.

The contours for GX 339–4 (a black-hole candidate, see, e.g., Z98) are shown in Figs. 4a, c. We see a very strong $R(\Gamma)$ correlation in 5 observations of this object (as found by Ueda et al. 1994). Also, Fig. 4c shows 3 contours for *Ginga* observations of Nova Muscae 1991 in the hard state (Życki et al. 1998). We see an $R(\Gamma)$ correlation (as found by Życki et al. 1999) indistinguishable from that in GX 339–4.

As argued in ZLS99, the presence of the correlation implies a feedback in which the presence of the reflecting cold medium affects the hardness of the X-ray spectra. A natural explanation for the feedback is that the cold medium emits soft photons irradiating the X-ray source and serving as seeds for thermal-Compton upscattering. Then, the larger the solid angle subtended by the reflector, the stronger the flux of soft photons, and, consequently, the stronger cooling of the thermal plasma. In a thermal plasma, the larger the cooling rate, the softer the resulting X-ray power-law spectra. The evidence that the Xγ spectra of both Seyferts and black-hole binaries in the hard state are indeed formed by thermal Comptonization (Gierliński et al. 1997; Johnson et al. 1997; Grove

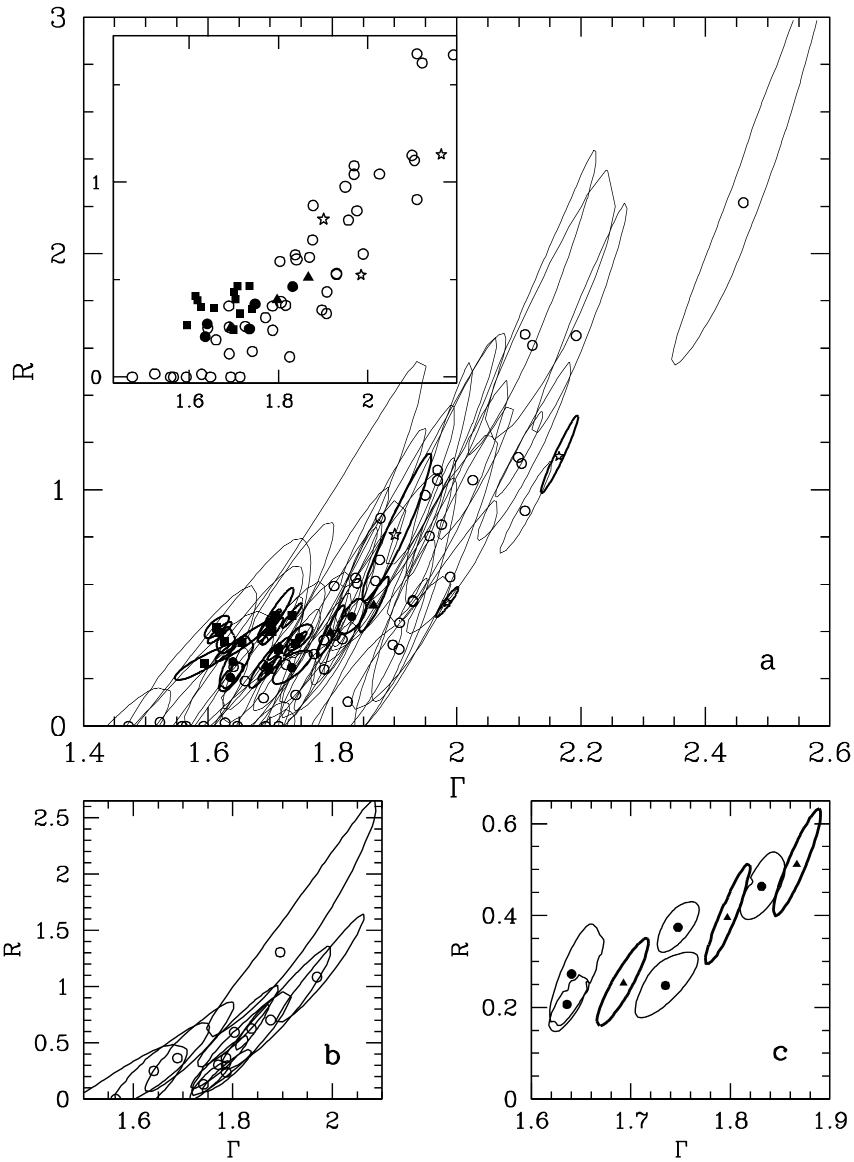

Figure 4. (a) The correlation of Compton reflection with the intrinsic X-ray spectral index in Seyferts (thin contours) and X-ray binaries in the hard state (heavy contours). Open circles correspond to Seyferts, and filled squares, circles, and triangles correspond to Cyg X-1, GX 339–4, and Nova Muscae 1991, respectively. Asterisks correspond to 3 observations of 2 X-ray bursters. The inset shows the best-fit points without error contours. (b) Similar correlation occurring in multiple observations of NGC 5548 and (c) GX 339–4 (thin contours and circles) and Nova Muscae 1991 (heavy contours and triangles).

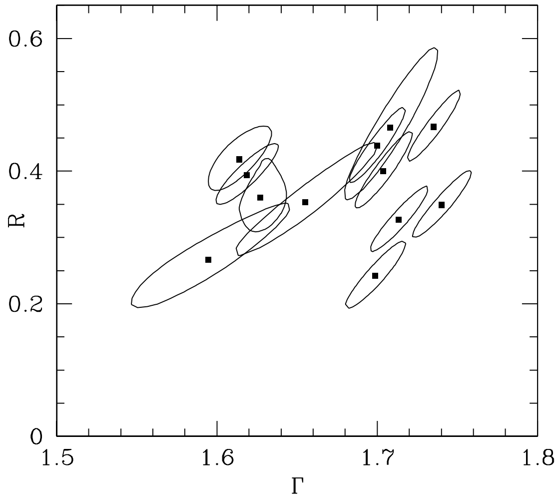

Figure 5. The strength of Compton reflection in *Ginga* observations of Cyg X-1 (assuming inclination of the reflecting disk of 30°).

et al. 1998; Zdziarski et al. 1996, Z97, Z98; see §§2, 3 above) strongly supports this explanation. On the other hand, models with X-ray emission being due to non-thermal electrons singly scattering seed photons would yield no dependence of the X-ray slope on the cooling rate (e.g. Lightman & Zdziarski 1987). Also, models with seed photons being mainly due to a process intrinsic to the hot plasma, e.g. thermal synchrotron radiation, would not reproduce the observed correlation.

Thus, the presence of the correlation implies that both the X-ray emitting plasma is thermal and that a substantial fraction of its cooling is due to soft photons coming from the cold matter responsible for the observed Compton reflection. Within this general model, various specific geometries can in principle reproduce the observational data presented in Fig. 4. This issue is discussed in §6 below.

In Fig. 4a, we see that Compton reflection in Cyg X-1, although with moderate R, is still significantly stronger than reflection for Seyferts at the corresponding range of Γ. The contours of the reflection strength in the 12 *Ginga* observations of Cyg X-1 in 1987, 1990 and 1991 are also shown separately in Fig. 5. We note that these contours have been obtained assuming the source inclination of 30°. If the actual inclination is larger (Done & Życki 1999), the values of R implied by the data would further increase. We also see in Figs. 4a, c that the strengths of Compton reflection in GX 339–4 and Nova Muscae 1991 are at least equal to the average R of Seyferts. Thus, Compton reflection in black-hole binaries does *not* appear to be anomously weak. Rather, reflection at a given Γ is stronger on average in black-hole binaries than in Seyferts.

This fact can be naturally explained in the framework of the model with thermal Comptonization of blackbody photons emitted by the reflecting medium, e.g. an optically-thick accretion disk. The difference between sizes of stellar-mass and supermassive black-hole sources implies different typical energies of black-body photons. In inner disks around stellar-mass black holes, they are in the soft X-ray range whereas they are in the UV range in the case of supermassive black holes. Sources with the same strength of reflection are likely to have similar relative geometries of the hot plasma and the cold medium, and thus similar ratios of the fluxes in the hard, Compton-upscattered, radiation to those in soft, seed, photons incident on the hot plasma. This ratio is equal to the amplification factor, A, of the Comptonization process.

The X-ray spectral index, Γ, depends in general on A, in the sense that the larger A, the harder the spectrum. However, Γ depends also on the ratio of the plasma temperature, T, to the characteristic temperature of the seed photons, $T_{\rm seed}$. As discussed above, typical plasma temperatures are similar in black-hole binaries and in Seyferts. Then, at the constant T, the larger $T_{\rm seed}$, the harder the X-ray spectrum (see Beloborodov 1999b). As seen in Fig. 4a, this effect is seen in the data. For a given R, black-hole sources have smaller Γ on average, i.e., harder X-ray spectra. In §6 below, the data are compared with theoretical predictions for $R(\Gamma)$ at two values of $T_{\rm seed}$ for a specific source geometry.

5. X-ray and Soft Gamma-ray Spectra of Radio Galaxies

As it is well established by now, Xγ emission of blazars is strongly beamed and originates in their powerful jets (e.g. Sikora 1997). The jets and their lobes are also responsible for the strong radio emission of that class of objects. An interesting issue regards their nuclear, unbeamed, Xγ emission. In blazars, the Xγ emission of jets (oriented close to line of sight) is so strong that it dominates completely any nuclear Xγ component. To study the latter, we thus have to turn to radio-loud AGNs with jets oriented at a significant angle with respect to the line of sight.

One suitable class of objects is nearby BLRGs. Xγ emission of a sample of them (3C 111, 3C 120, 3C 382, 3C 390.3, 3C 445) has recently been studied by W98. These authors used spectral data from *Ginga*, *ASCA*, *EXOSAT*, and OSSE. Their main findings are summarized below.

First, the intrinsic X-ray spectra of BLRGs are harder and their reflection components are weaker than those typical for RQ Seyferts. For example, the average *Ginga* spectrum of 4 of the above BLRGs has $\Gamma = 1.67^{+0.05}_{-0.04}$, $R = 0.08^{+0.17}_{-0.08}$, while we see in Fig. 4a that Seyferts have $\Gamma \sim 2$, $R \sim 1$ on average. On the other hand, ZLS99 found that this difference does not imply that BLRGs and RQ Seyferts belong to two different populations as far as their Γ and R are concerned. Rather, BLRGs occupy a part of the Γ-R parameter space also populated by RQ Seyfert 1s. This is shown in Fig. 6, which shows the error contours for BLRGs and the nearby obscured radio galaxy Cen A in comparison to the best-fit points for RQ Seyferts.

Second, *ASCA* observations of those objects show that their Fe Kα lines are relatively weak and narrow. The observed profiles are shown in Fig. 7. In all cases except 3C 120, the intrinsic line widths are consistent with null within 90% confidence (see Table 10 in W98). In the case of 3C 120 fitted with a broken power-law continuum without reflection and a Gaussian line, both the line width, $\sigma_{\rm Fe} = 0.32^{+0.76}_{-0.20}$ keV, and the equivalent width, $W_{\rm Fe} \simeq 100$ eV, are

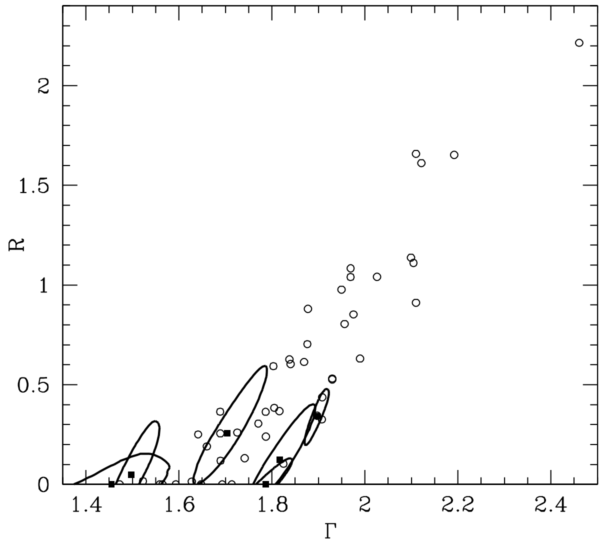

Figure 6. Compton reflection in radio galaxies observed by *Ginga* (fileed squares and contours) in comparison to that in RQ Seyferts (open circles).

moderate. Inclusion of reflection (not constrained by the *ASCA* data) would reduce the fitted $\sigma_{\rm Fe}$ and $W_{\rm Fe}$.

The Fe Kα lines, although moderate, have still been found by W98 too strong to be accounted for by the observed weak Compton reflection. To solve this problem, W98 proposed that a large fraction of the line flux originates in a medium with the column density, $N_{\rm H}$, being $< 10^{24}$ cm^{-2}, e.g. a molecular torus surrounding the nucleus. The Thomson optical depth of such a medium is then < 1, and its Compton reflection does not give a hump above ~ 10 keV (W98), characteristic to reflection from optically-thick media. On the other hand, such a medium still can produce observable Fe Kα lines. It can be estimated that for a solid angle of $\sim 2\pi$ subtended by that medium as seen from the central source, an $N_{\rm H} \sim 10^{23}$ cm^{-2} is required to account for the observed line fluxes above those due the observed Compton reflection (W98). A medium with such $N_{\rm H}$ is, in fact, observed in absorption in 3C 445 (as well as in Cen A).

We note that the results of W98 regarding the strength and the width of the Fe Kα lines in BLRGs differ from those of Reynolds (1997), Grandi et al. (1997) and Nandra et al. (1997), who generally found the lines to be stronger and broader. Some of the differences are accounted for by improvements in the calibration of *ASCA*. Those authors used its version of 1995 or earlier whereas W98 used the release of 1997. The effect of this change in the *ASCA* response and effective area can be illustrated by a comparison of fits with the same model (power law plus a Gaussian line) to the same *ASCA* spectrum of 3C 120 fitted in the 3–10 keV range. For that spectrum, Nandra et al. (1997) obtain $\sigma_{\rm Fe} = 0.74^{+0.34}_{-0.27}$ keV, $W_{\rm Fe} = 330^{+200}_{-120}$ eV, whereas W98 obtain $\sigma_{\rm Fe} = 0.28^{+0.96}_{-0.16}$

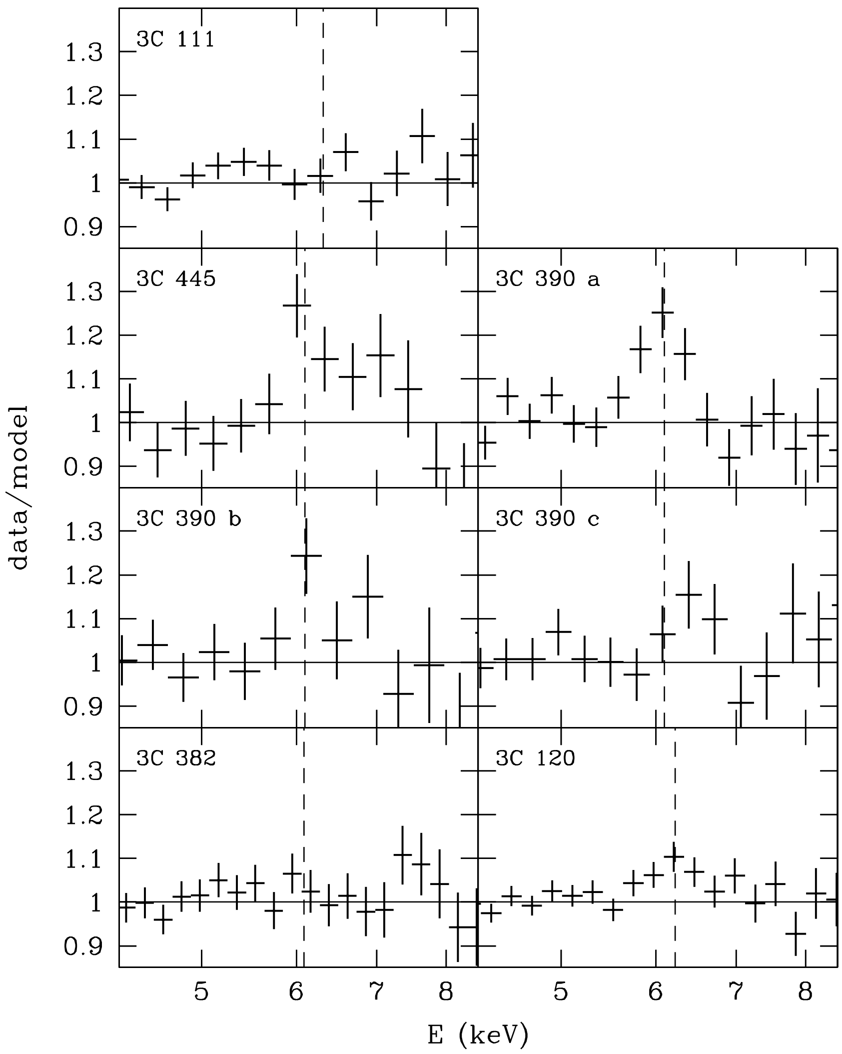

Figure 7. Fe Kα line profiles of BLRGs observed by *ASCA*, as analyzed by W98.

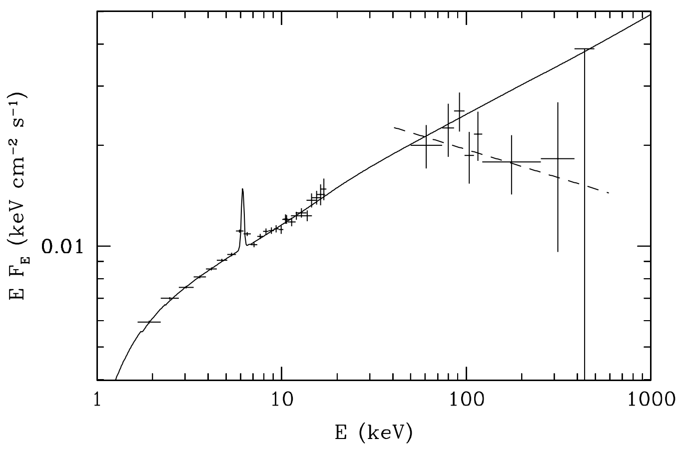

Figure 8. The average Xγ spectrum of BLRGs from *Ginga* and OSSE. The solid curve gives the best fit of a model with power law and (weak) Compton reflection to the *Ginga* data, and the dashed curve gives the power-law fit to the OSSE data.

keV, $W_{\rm Fe} \approx 100$ eV. Further, some of those authors fitted the entire energy range of *ASCA*, ~ 0.5–10 keV, with a single power-law continuum. This neglects the soft excess, which was found below ~ 3 keV in most observations of BLRGs in W98. Given the limited effective area of *ASCA* above 7 keV, the claimed huge lines (e.g. with $\sigma_{\rm Fe} \approx 2$ keV and $W_{\rm Fe} \approx 1$ keV in 3C 120 and 3C 382) are artifacts of compensating for the underestimated continuum at $\gtrsim 6$ keV, with the underestimation due to fitting a single power law to a concave intrinsic spectrum (W98).

The findings of W98 are consistent with results of Eracleous & Halpern (1998) for the BLRG Pictor A. They find no detectable Fe Kα line in the *ASCA* spectrum of that object, similarly to the case of 3C 111 (Fig. 7). Although *ASCA* data alone cannot determine the strength of reflection, no detectable Fe Kα line is compatible with $R \ll 1$ in Pictor A. Also, its power-law X-ray index, $\Gamma \simeq 1.76 \pm 0.05$, is consistent with the range of Γ found in BLRGs in W98 (see Fig. 6).

W98 also studied the broad-band Xγ spectra of BLRGs. Those spectra break and become softer above ~ 100 keV, as shown by a simultaneous *ASCA*/OSSE observation of 3C 120 and by the OSSE spectra being on average much softer than the X-ray spectra. Fig. 8 shows the average Xγ spectrum of BLRGs from *Ginga* and OSSE (W98). The energy of the break is similar to that seen in RQ Seyferts (§§2, 3). Also, the (Γ, R) space occupied by BLRGs lies within that covered by RQ Seyferts, as shown in Fig. 6. The above facts support the origin of the Xγ spectra of BLRGs from thermal Comptonization, similarly as it seems to be the case for RQ Seyferts.

On the other hand, the average OSSE spectrum of BLRGs does not show a curvature, see Fig. 8 (in contrast to that of RQ Seyferts), which allows for an origin of Xγ photons from non-thermal Comptonization. This conjecture appears to be supported by the form of the broad-band Xγ spectrum of Cen A. In X-rays, $\Gamma \approx 1.7$–1.8 (W98; Steinle et al. 1998) and $R = 0^{+0.15}$ (W98), i.e., very similar to spectra of BLRGs. The spectrum breaks to a softer power law with $\Gamma \gtrsim 2$ above 150 keV, and then it breaks again above ~ 10 MeV, to $\Gamma \gtrsim 3$, as required by an EGRET detection of the source in the 0.1–1 GeV energy range (Steinle et al. 1998). Observations of photons at such high energies indicate the presence of non-thermal electrons in the Xγ source of Cen A. The data on BLRGs are of much more limited statistics and the issue whether their Xγ spectra are from thermal Comptonization or a non-thermal process remains open so far.

6. Geometry

Results presented above show that the Xγ spectra of black-hole binaries in the hard state are similar to those of Seyferts, and probably to those of BLRGs. This suggests a source geometry common to those sources. Within that geometry, at least one variable parameter is required to account for the X-ray hardness and the associated strength of Compton reflection varying from source to source (as well as being variable in some individual objects).

Currently, there are two main competing pictures of the geometry of central regions of black-hole binaries in the hard state and Seyferts. In one picture, the Xγ source forms a central hot disk (Shapiro, Lightman & Eardley 1976). The plasma in that disk is two-temperature, with ions being much hotter than the electrons, and with Coulomb energy transfer from the former to the latter. The accretion-disk solution of Shapiro et al. (1976) is cooling-dominated and it has been found thermally unstable by Pringle (1976). However, there exists another solution, dominated by advection of hot ions into the black hole, which seems to be stable (Abramowicz et al. 1995; Narayan & Yi 1995). The intersection of the two solutions corresponds to the maximum possible accretion rate and luminosity from the system. As discussed, e.g., by Zdziarski (1998), typical temperature and optical depth in the vicinity of that maximum are $kT \sim 100$ keV, $\tau \sim 1$, which are just the average values observed from Seyfert 1s and black-hole binaries in luminous hard states (see §§2, 3 above).

Observations of Compton reflection accompanying thermal Comptonization imply the presence of optically-thick medium in the vicinity of the hot disk. This might be a standard optically-thick disk (Shakura & Sunyaev 1973) surrounding the hot disk. In general, there may be an overlap between the two phases.

We consider an idealized model of a central optically-thin sphere of unit radius surrounded by a flat, cold, disk partly embedded in the hot sphere (Fig. 9). There is no intrinsic dissipation in the disk, the hot sphere radiates via thermal Comptonization, and the seed photons for upscattering are only the reprocessed ones emitted by the disk. The relative overlap of the hot and cold phases (as given by the radius d) determines then the X-ray slope of the spectrum. When $d \gtrsim 1$, both cooling and the strength of reflection are weak, and both increase with decreasing d. This simple model can be compared to the values of Γ and R observed in Seyferts and hard-state black-hole binaries (ZLS99; §4), as shown by the dotted curve in Fig. 10 (for which $T_{\rm seed} = 5$ eV was assumed). We see that this model reproduces the data for $R \leq 1$ reasonably well.

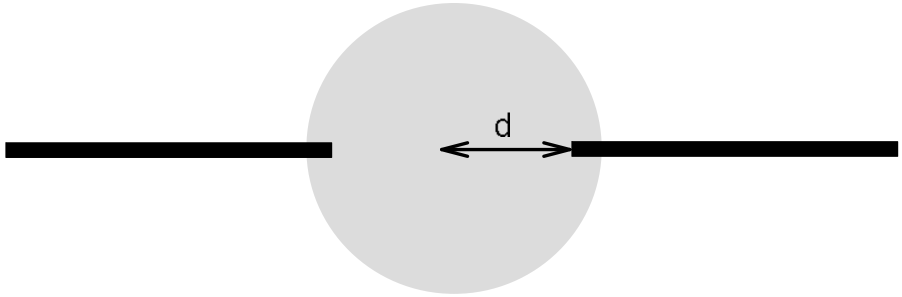

Figure 9. The geometry with a central hot plasma surrounded by a cold disk. The cold disk enters partly the hot plasma down to the radius d, which parameter determines the spectral hardness and the amount of reflection present.

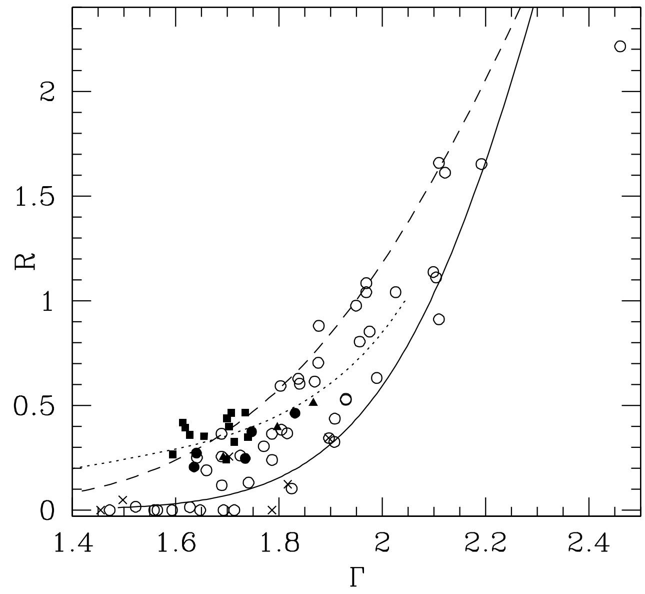

Figure 10. The R-Γ data together with model dependences for an inner hot/outer cold disks (dotted curve), and for mildly-relativistic bulk motion of the hot plasma above a cold disk in the cases of seed photons at $kT_{\rm seed} = 5$ eV and 200 eV (solid and dashed curves, respectively). Open circles and crosses correspond to Seyferts and radio galaxies, respectively, and filled square, circles and triangles, to Cyg X-1, GX 339–4 and Nova Muscae 1991, respectively.

On the other hand, this simple model neglects the effect of Compton upscattering of the reflected radiation in the hot plasma, which would then reduce R significantly, especially for $d \lesssim 1$. This effect has been taken into account, e.g., in models of Esin et al. (1997, 1998) and Z98. Their general finding is that the strength of Compton reflection predicted in those models is weaker than that observed in black-hole binaries. The reflection strength would increase in the presence of disk flaring. Flaring is, in fact, predicted by the standard model of Shakura & Sunyaev (1973), and it is further enhanced by irradiation (e.g. Vrtilek et al. 1990). However, these effects have been taken into account in the model of the hard state of Cyg X-1 by Esin et al. (1998), who found the predicted reflection strength still less than that observed.

This might be less of a problem for Seyferts with hard spectra, which often have weak or null reflection, see Fig. 10. On the other hand, there are Seyferts with soft spectra and strong reflection, $R \sim 2$ (and strong accompanying Fe Kα lines), e.g. MCG –6-30-15. If their geometry is similar to that shown in Fig. 9 for $d \ll 1$, R has to be < 1. In Seyferts, R can be increased by both disk flaring and additional reflection from Thomson-thick molecular torii surrounding the central source (Ghisellini, Haardt & Matt 1994; Krolik, Madau & Życki 1994). However, these effects should also be effective in some Seyferts with hard spectra, contrary to the data in Fig. 10 showing absence of Seyferts with substantial reflection at $\Gamma \lesssim 1.6$. Thus, the presence of reflection with $R > 1$ in some unobscured Seyferts is a problem for this model. (If the primary source is obscured but a part of the reflector is not, $R \gg 1$ can be observed, e.g. Reynolds et al. 1994.)

Coming back to black-hole binaries, their models in terms of a hot inner disk and an outer cold disk with a variable inner radius are supported by findings of Życki, Done & Smith (1998) and Done & Życki (1999), who consider the effect of relativistic smearing of both Compton reflection and the accompanying Fe Kα line. The smearing occurs due to rotation of the disk in the gravitational potential of the black hole (e.g. Fabian et al. 1989), and it can be used to measure the range of radii where Compton reflection takes place. Życki et al. (1998) and Done & Życki (1999) find that the observed reflection strength, R, roughly anticorrelates with the inner radius of the cold disk (as inferred from relativistic smearing) in Nova Muscae and Cyg X-1. This is consistent with the source geometry shown in Fig. 9.

The other geometry proposed for the Xγ sources in accreting black holes is that of an active corona above the surface of an accretion disk. A likely mechanism of energy dissipation in this case is magnetic flares (Galeev, Rosner & Vaiana 1979; B99a). Haardt & Maraschi (1993) proposed a model with a homogeneous corona. This model can work for soft sources provided the corona optical depth is $\ll 1$, as to avoid strong attenuation of both reflection and the Fe Kα line due to scattering by hot electrons in the corona. A modified model with localized active regions (Haardt, Maraschi & Ghisellini 1994) works well for objects with average Γ and R (Stern et al. 1995). However, it can be ruled out for black-hole binaries in the hard state (Gierliński et al. 1997; Z98). The hard X-ray spectra of these objects require the active regions to be elevated above the disk to reduce cooling, which, however, results in $R \sim 1$, i.e., more than observed.

A solution to this problem has been proposed by B99a. Namely, he postulates that the active regions have some bulk motion, which can be due to the pressure of reflected radiation and/or plasma ejection from magnetic flares. A mildly relativistic flow away from the disk, with a velocity βc, reduces then the downward Xγ flux, which in turn reduces both reflection and reprocessing. The reduction of the reprocessed flux incident on the hot plasma leads to a spectral hardening (analogously to the previous model). Two $R(\Gamma)$ dependences of this model (for $i = 30^\circ$ and for a geometry-dependent parameter of B99a of $\mu_{\rm s} = 0.4$) are shown in Fig. 10. The solid and dashed curves correspond to seed photons at $kT_{\rm seed} = 5$ eV and 200 eV, characteristic to Seyferts and black-hole binaries, respectively. A given R corresponds to the same β on both curves. E.g., $R = 0.3$, 0.5, 1, and 1.5 correspond to $\beta = 0.27$, 0.15, 0, and -0.10 (i.e., flow towards the disk), respectively. We see that the dashed curve reproduces quite well the data for black-hole binaries. The solid curve reproduces well the data for Seyferts with softest spectra for given R. Then variations in the orientation, energy of the seed photons, and the plasma parameters from source to source can reproduce the width of the correlation. A model best-fitting the Seyfert data is shown in Beloborodov (1999b) and ZLS99. Comparing the solid and dashed curves, we also see that different values of $T_{\rm seed}$ can indeed explain the black-hole binaries being harder on average than Seyferts, as discussed at the end of §4.

Outflows were also proposed by W98 to explain the weakness of reflection in radio galaxies. We see that indeed the low-$T_{\rm seed}$ model of B99a explains well those data (solid curve and crosses in Fig. 10).

Outflows cannot, of course, explain the data with $R > 1$. On the other hand, a mildly relativistic motion directed towards the disk will enhance reflection and cooling, leading to soft spectra with $R > 1$, as also proposed by B99a. Possibly, such downward motion can be due to ejection of plasma blobs from magnetic flares towards the disk. As seen in Fig. 10, the model of B99a appears in principle capable to explain the entire observed correlation.

7. Conclusions

A general picture of Xγ sources in Seyferts and black-hole binaries in the hard state that emerges from the results presented above is of a hot thermal plasma with $kT \sim 10^2$ keV and $\tau \sim 1$ located in the vicinity of a cold, optically-thick, medium. The main radiative process in the hot plasma is Compton upscattering of some soft seed photons. The X-ray slope of Compton-upscattered photons depends on the rate of cooling of the hot plasma by the soft photons.

If the seed photons are emited by the reflecting medium, the strength of the coupling determines the specific shape of emitted Xγ spectra. When the coupling between the hot and cold media is weak, there are few soft photons incident on the hot plasma, which results in weak cooling and hard spectra. Also, few hard photons from the hot plasma are incident on the cold medium and Compton reflection is weak. On the other hand, when the coupling is strong, the plasma cooling is also strong, which yields soft X-ray slopes. Also, many hard photons are incident on the cold medium and reflection is strong. This explains the strong correlation between the intrinsic X-ray spectral index and the relative strength of reflection found by ZLS99 (§4).

This general picture appears to be consistent with two geometries. One is of a hot inner disk surrounded by a cold outer disk. The amount of overlap between the hot and cold phases determines then the strength of the coupling (Fig. 9). The other is of a hot plasma blob above the surface of a cold disk moving perpendicular to the disk. In the case of mildly relativistic outflow, the coupling is weak, whereas motion towards to the disk leads to a strong coupling. Current data appear insufficient to conclusively determine which of these geometries applies to observed black-hole sources.

Some differences between different classes of sources can be explained within the above scenario. Namely, the black-hole binaries have their intrinsic spectra harder than Seyferts for given reflection strength, R. This is likely to be due the different characteristic blackbody energies in stellar-mass systems and around supermassive black holes. The higher blackbody energies in black-hole binaries lead then to harder spectra for given amplification of seed photons by thermal Comptonization (§§4, 6). The hard spectra and weak reflection of BLRGs can be then connected to either relativistic outflows of the hot plasma or due to the cold disks terminating far away from the central black hole in those sources.

Acknowledgments. I thank Andrei Beloborodov for valuable discussions, and Ken Ebisawa and Piotr Życki for providing me with their *Ginga* data on Cyg X-1 and Nova Muscae 1991, respectively. This research has been supported in part by the KBN grants 2P03C00511p0(1,4) and 2P03D00614, and NASA grants and contracts.

References

Abramowicz M. A., Chen X., Kato S., Lasota J.-P., Regev O., 1995, ApJ, 438, L37

Beloborodov A. M., 1999a, ApJ, 510, L123 (B99a)

Beloborodov A. M., 1999b, in High Energy Processes in Accreting Black Holes, J. Poutanen & R. Svensson, Provo: ASP Conf. Series, this volume

Brandt S., 1997. Statistical and Computational Methods in Data Analysis, 3rd ed., New York: Springer

Cropper M., Ramsey G., Wu K., 1998, MNRAS, 293, 222

Done C., Magdziarz P., 1998, MNRAS, 298, 737

Done C., Osborne J. P., 1997, MNRAS, 288, 649

Done C., Życki P. T., 1999, MNRAS, in press

Done C., Mulchaey J. S., Mushotzky R. R., Arnaud K. A., 1992, ApJ, 395, 275

Done C., Osborne J. P., Beardmore A. P., 1995, MNRAS, 276, 483

Ebisawa K., Ueda Y., Inoue H., Tanaka Y., White N. E., 1996, ApJ, 467, 419

Eracleous M., Halpern J. P., 1998, ApJ, 505, 577

Esin A. A., McClintock J. E., Narayan R., 1997, ApJ, 489, 865

Esin A. A., Narayan R., Cui W., Grove J. E., Zhang S.-N., 1998, ApJ, 505, 854

Fabian A. C., Rees M. J., Stella L., White N. E., 1989, MNRAS, 238, 729

Galeev A. A., Rosner R., Vaiana G. S., 1979, ApJ, 229, 318

George I. M., Fabian A. C., 1991, MNRAS, 249, 352

Ghisellini, G., George, I. M., Fabian, A. C., Done C. 1990, MNRAS, 248, 14

Ghisellini, G., Haardt F., Matt G., 1994, MNRAS, 267, 743

Gierliński M., Zdziarski A. A., Done C., Johnson W. N., Ebisawa K., Ueda Y., Haardt F., Phlips B. F., 1997, MNRAS, 288, 958

Gierliński M., Zdziarski A. A., Poutanen J., Coppi P. S., Ebisawa K., Johnson W. N., 1999, MNRAS, in press

Gondek D., Zdziarski A. A., Johnson W. N., George I. M., McNaron-Brown K., Magdziarz P., Smith D., Gruber D. E., 1996, MNRAS, 282, 646

Grandi P., Sambruna R. M., Maraschi L., Matt G., Urry C. M., Mushotzky R. F., 1997, ApJ, 487, 636

Grove J. E., Johnson W. N., Kroeger R. A., McNaron-Brown K., Skibo J. G., 1998, ApJ, 500, 899

Haardt F., Maraschi L., 1993, ApJ, 413, 507

Haardt F., Maraschi L., Ghisellini G., 1994, ApJ, 432, L95

Johnson W. N., McNaron-Brown K., Kurfess J. D., Zdziarski A. A., Magdziarz P., Gehrels N., 1997a, ApJ, 482, 173

Johnson W. N., Zdziarski A. A., Madejski G. M., Paciesas W. S., Steinle H., Lin Y.-C., 1997b, in The 4th Compton Symposium, C. D. Dermer, M. S. Strickman, & J. D. Kurfess, AIP Conf. Proc. Vol. 410, Woodbury, 283

Krolik J. H., Madau P., Życki P., 1994, ApJ, 420, L57

Lee J. C., Fabian A. C., Reynolds C. S., Iwasawa K., Brandt W. N., 1998, MNRAS, 300, 583

Lightman A. P., White T. R., 1988, ApJ, 335, 57

Lightman A. P., Zdziarski A. A., 1987, ApJ, 319, 643

Magdziarz P., Zdziarski A. A., 1995, MNRAS, 273, 837

Magdziarz P., Blaes O. M., Zdziarski A. A., Johnson W. N., Smith D. A., 1998, MNRAS, 301, 179

Nandra K., Pounds K. A., 1994, MNRAS, 268, 405

Nandra K., George I. M., Mushotzky R. F., Turner T. J., Yaqoob T., 1997, ApJ, 477, 602

Narayan R., Yi I., 1995, ApJ, 452, 710

Phlips B. F., et al. 1996, ApJ, 465, 907

Pounds K. A., Nandra K., Stewart G. G., George I. M., Fabian A. C., 1990, Nat, 344, 132

Pounds K. A., Done C., Osborne J. P., 1995, MNRAS, 277, L5

Poutanen J., 1998, in Theory of Black Hole Accretion Discs, M. A. Abramowicz, G. Björnsson, & J. E. Pringle, Cambridge: Cambridge Univ. Press, 100

Poutanen J., Coppi P. S., 1998, Physica Scripta, T77, 57

Poutanen J., Svensson R., 1996, ApJ, 470, 249

Poutanen J., Krolik J. H., Ryde F., 1997, in The 4th Compton Symposium, C. D. Dermer, M. S. Strickman, & J. D. Kurfess, AIP Conf. Proc. Vol. 410, Woodbury, 972

Pringle J. E., 1976, MNRAS, 177, 65

Reynolds C. S., 1997, MNRAS, 286, 513

Reynolds C. S., Fabian A. C., Makishima K., Fukazawa Y., Tamura T., 1994, MNRAS, 268, L55

Shakura N. I., Sunyaev R. A., 1973, A&A, 24, 337

Shapiro S. L., Lightman A. P., Eardley D. M., 1976, ApJ, 204, 187

Sikora M., 1997, in The 4th Compton Symposium, C. D. Dermer, M. S. Strickman, & J. D. Kurfess, AIP Conf. Proc. Vol. 410, Woodbury, 494

Smith D. A., Done C., 1996, MNRAS, 280, 355

Steinle H., et al.,1998, A&A, 330, 97

Stern B. E., Poutanen J., Svensson R., Sikora M., Begelman M. C., 1995, ApJ, 449, L13

Strickman M., Skibo J., Purcell W., Barret D., Motch C., 1996, A&AS, 120, (III)217

Tomsick J. A., Kaaret P., Kroeger R. A., Remillard R. A., 1999, ApJ, in press

Ueda Y., Ebisawa K., Done C., 1994, PASJ, 46, 107

Vrtilek S. D., Raymond J. C., Garcia M. R., Verbunt F., Hasinger G., Kürster M., 1990, A&A, 235, 162

Weaver K. A., Krolik J. H., Pier E. A., 1998, ApJ, 498, 213

Woźniak P. R., Zdziarski A. A., Smith D., Madejski G. M., Johnson W. N., 1998, MNRAS, 299, 449 (W98)

Yoshida K, Mitsuda K, Ebisawa K., Ueda Y., Fujimoto R., Yaqoob T., Done C., 1993, PASJ, 45, 605

Zdziarski A. A., 1998, MNRAS, 296, L51

Zdziarski A. A., Johnson W. N., Magdziarz P., 1996, MNRAS, 283, 193

Zdziarski A. A., Johnson W. N., Poutanen J., Magdziarz P., Gierliński M., 1997, in The Transparent Universe, C. Winkler, T. Courvoisier, & P. Durouchoux, ESA SP-382, 373 (Z97)

Zdziarski A. A., Poutanen J., Mikołajewska J., Gierliński M., Ebisawa K., Johnson W. N., 1998, MNRAS, 301, 435 (Z98)

Zdziarski A. A., Lubiński P., Smith D. A., 1999, MNRAS, in press (ZLS99)

Życki P. T., Done C., Smith D. A., 1998, ApJ, 496, L25

Życki P. T., Done C., Smith D. A., 1999, MNRAS, in press